

# Photoelectrochemical Behavior in Low-Conductivity Media of Nanostructured TiO<sub>2</sub> Films Deposited on Interdigitated Microelectrode Arrays

Robin Morand,<sup>†</sup> Christian Lopez,<sup>‡</sup> Milena Koudelka-Hep,<sup>§</sup> Piotr Kedzierzawski,<sup>||</sup> and Jan Augustynski<sup>\*,†</sup>

Department of Chemistry, University of Geneva, CH-1211 Geneva 4, Switzerland, Laboratoire d'Electrochimie et de Physico-chimie des Matériaux et des Interfaces, E.N.S.E.E.G., 38402 Saint Martin d'Hères, France, Institute of Microtechnology, University of Neuchâtel, 2007 Neuchâtel, Switzerland, and Institute of Physical Chemistry of Polish Academy of Sciences, 01-224 Warsaw, Poland

Received: February 21, 2002; In Final Form: May 17, 2002

Mesoporous titanium dioxide films were electrophoretically deposited from colloidal suspensions in water on interdigitated microelectrode arrays and also on conducting glass substrates. Even unsintered (just dried) TiO<sub>2</sub> films exhibit already usual photocurrent–voltage behavior. Due to the reduced ohmic losses typical of the microelectrode arrays, the effect of the ionic strength of the aqueous electrolyte upon photooxidation of an uncharged hole scavenger (methanol) could be examined. A consistent slight increase of the saturation photocurrent accompanying decreasing concentration of the supporting electrolyte was observed. Measurements performed in various water/methanol mixtures showed a marked continuous increase of the photoresponse with increasing concentration of the dominant hole scavenger (i.e., methanol), suggesting its adsorption as the rate-determining step of the photooxidation process. Close proximity of the TiO<sub>2</sub> microanodes and Pt microcathodes, separated by 5  $\mu\text{m}$  gaps, enabled us also to monitor the interplay between the oxygen reduction and the photooxidation of methanol. Accordingly, the presence of oxygen in the solution caused a dramatic decrease of the photocurrent apparently reflecting the effect of hydrogen peroxide, formed at the microcathodes, acting as particularly efficient scavenger of the conduction band electrons at the TiO<sub>2</sub> microanodes. In fact, the observed methanol oxidation photocurrents were only slightly affected by the presence of oxygen when the microcathodes were disconnected and replaced by a few millimeter distant external macrocathode. Experiments involving solutions of a large series of organic compounds in pure water revealed a variety of behaviors going from a highly efficient photooxidation to a virtual suppression of the photocurrent. Apparently, the compounds belonging to the latter category, such as acetone and acetophenone, undergo strong adsorption at the TiO<sub>2</sub> surface blocking, when present in large concentration, most of the active sites on the surface of the photocatalyst.

## Introduction

Among a variety of compound semiconductors, titanium dioxide is by far the most frequently used as photocatalyst.<sup>1–5</sup> This is due to its good long-term stability, high oxidizing power and, importantly, to the appropriate position of its conduction band allowing oxygen to act as acceptor of photogenerated electrons. In the case of water treatment applications, colloidal TiO<sub>2</sub> powders are employed either as suspensions or, alternatively, are immobilized on various solid supports to form films or ceramic membranes.<sup>2,5</sup> Such large-surface-area porous TiO<sub>2</sub> coatings are also used for photocatalytic oxidation of different gas-phase contaminants.<sup>2,6</sup> In most of the practical situations, such TiO<sub>2</sub> photocatalyst operates in low conductivity media, i.e., either in the presence of small amounts of an electrolyte or in its virtual absence. This makes separate electrochemical investigation of partial photoanodic and partial cathodic processes involved in the photocatalytic reactions uneasy. Another domain in which application of mesoporous TiO<sub>2</sub> films has led

to important practical developments is that of liquid-junction dye-sensitized photovoltaic cells.<sup>7,8</sup>

The mechanism by which such films formed by a network of interconnected TiO<sub>2</sub> nanoparticles (employed either under band gap UV illumination or sensitized with visible light absorbing dyes) ensure an efficient collection of photogenerated electrons at the back contact has been the subject of numerous studies.<sup>9,10</sup> One of important questions concerns the exact role played by the electrolyte, filling the pores of the film, in the charge transport in such a system. The presence of an electrolyte in the pores makes, in particular, possible the net charging of the film under external polarization, such excess of charge being compensated by the ions of the supporting electrolyte.<sup>11,12</sup> A direct relationship between the charge transport in nanostructured films and the conductivity of the electrolyte has been inferred from transient photocurrent measurements.<sup>10</sup>

Here we describe the preparation and compare the photoelectrochemical characteristics of nanostructured TiO<sub>2</sub> films formed by electrophoretical deposition either on conventional conducting glass substrates or on interdigitated microelectrode arrays (IDAs) including Ti/Ti and/or Ti/Pt electrode pairs. We have chosen this particular microelectrode geometry,<sup>13</sup> allowing among others to minimize solution resistance effects, to examine

\* Corresponding author. E-mail: Jan.Augustynski@chiam.unige.ch.

<sup>†</sup> University of Geneva.

<sup>‡</sup> Laboratoire d'Electrochimie et de Physico-chimie des Matériaux et des Interfaces, E.N.S.E.E.G.

<sup>§</sup> University of Neuchâtel.

<sup>||</sup> Institute of Physical Chemistry of Polish Academy of Sciences.

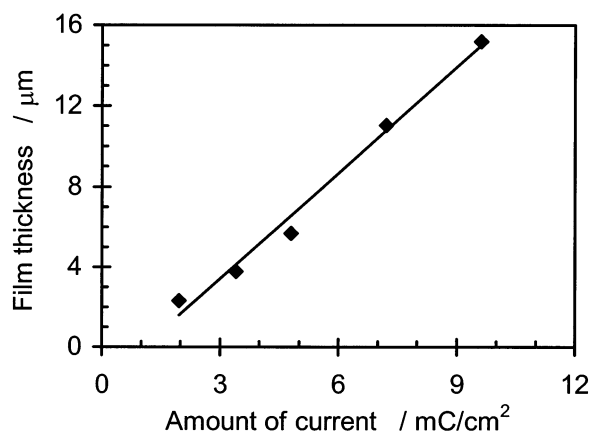


**Figure 1.** Thickness of TiO<sub>2</sub> films deposited at conducting glass substrates plotted against the amount of electrophoresis current.

the photoelectrochemical behavior of nanostructured TiO<sub>2</sub> films in solutions of varying ionic strength and also in various organic solvents, pure or dissolved in water (in the absence of other redox species and without a supporting electrolyte).

### Experimental Section

**Deposition of TiO<sub>2</sub> Films by Electrophoresis.** The nanostructured TiO<sub>2</sub> films were formed by cathodic electrophoretic deposition using a 0.25% suspension of TiO<sub>2</sub> (P25 from Degussa: 80% anatase, 20% rutile) in water. Before addition of the TiO<sub>2</sub> powder, ultrapure (Millipore Milli-Q) water was saturated with CO<sub>2</sub> in order to make it slightly acidic and to allow the TiO<sub>2</sub> particles to become positively charged (note that the values of the point of zero charge, PZC, of anatase reported in the literature range from pH 6.0 to pH 6.4 and those for rutile are only slightly lower<sup>14</sup>). The fresh suspension was stirred for half an hour and sonicated for at least 1 h before use. The electrophoretic deposition at conducting glass substrates (Libbey Owens Ford, 12 Ω/square, comprising a 0.5 μm thick overlayer of F-doped SnO<sub>2</sub>) of ca. 1 cm<sup>2</sup> surface area was carried out against a large Pt anode distant 12 mm by applying a 4 V bias. As shown in Figure 1 the thickness (determined with a Tencor Alpha Step 200 profilometer) of the resulting TiO<sub>2</sub> films followed essentially the amount of the passed current. As deposited films were first dried in ambient air and then heated for 1 h at temperatures ranging from 100 to 500 °C. The electrophoresis was also employed to form the TiO<sub>2</sub> films at interdigitated microelectrode arrays. The corresponding IDAs were fabricated on Si/Si<sub>3</sub>N<sub>4</sub> wafers as described in detail elsewhere.<sup>15</sup> The interdigitated structures featured 1 mm long Ti microelectrode bands of a 5 μm width separated by 5 μm gaps. The total area of 50 microelectrode pairs was 0.5 mm<sup>2</sup>. In some cases one set of microelectrodes was covered with electrodeposited platinum. The selective deposition of TiO<sub>2</sub> nanoparticles at the chosen set of microelectrode bands was realized using the second set of interdigitated bands as local anodes in addition to an external 1 cm<sup>2</sup> Pt anode placed parallel to and 5 mm apart from the IDA. Both anodes were connected to the same terminal of the potentiostat and a bias of 2 V was applied during a short time, to reach the amount of charge ranging from 10 to 30 μC, resulting in a 100–200 nm thick TiO<sub>2</sub> deposit. Once the deposition finished, the IDA was immersed in ultrapure water when still maintaining the bias and slowly moved in the water. The bias was switched off only after this rinsing sequence and the IDA was allowed to dry at 100 °C for 1 h.

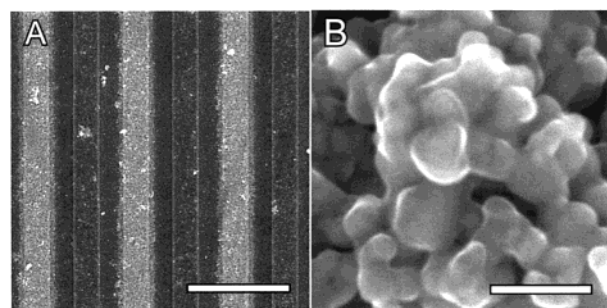


**Figure 2.** (A) SEM image of the IDA structure showing a set of 3 microbands bearing a TiO<sub>2</sub> deposit; bar length 20 μm. (B) Detailed SEM view of the TiO<sub>2</sub> deposit; bar length 100 nm.

Scanning electron microscopy (SEM) images of TiO<sub>2</sub> films were taken at 30 kV accelerating voltage in a Hitachi S-900 “in-lens” field-emission microscope.

**Photoelectrochemical Measurements.** The films were tested for their photoelectrochemical activity in a two-compartment Teflon cell equipped with a quartz window, by illuminating the TiO<sub>2</sub> electrode from the side of the film/solution interface. A large area platinum foil served as a counter-electrode and the potential of the TiO<sub>2</sub> electrode was monitored either versus a silver chloride/silver reference electrode or, in some cases, versus a silver pseudo-reference electrode. The TiO<sub>2</sub> films were illuminated with a 150 W xenon lamp equipped with a series of neutral density filters and focused on ca. 0.3 cm<sup>2</sup> surface area of the sample. The wavelength photoresponse (i.e., incident photon-to-current conversion efficiency vs excitation wavelength) of the conventional size TiO<sub>2</sub> electrodes was determined using a 500 W xenon lamp (Ushio UXL-502HSO) set in an Oriel model 66021 housing and a Multispec 257 monochromator (Oriel) with a bandwidth of 4 nm. The absolute intensity of the incident light from the monochromator was measured with a model 730 A radiometer/photometer from Optronic Lab. The photoelectrochemical measurements were carried out at ca. 25 °C under potential-controlled conditions. Chemicals used in the present work were obtained from Fluka and Merck and were of the highest available purity. Aqueous solutions were prepared in Milli-Q water.

### Results and Discussion

In Figure 2A is displayed a scanning electron microscopic (SEM) image of a part of an IDA with three pairs of band electrodes (5 μm wide) covered with a mesoporous TiO<sub>2</sub> film. Apparently some TiO<sub>2</sub> particles are also present in the inter-electrode gap and on the Ti counter electrode. In part B of Figure 2 is shown a high-resolution SEM view of such a TiO<sub>2</sub> deposit consisting of a network of ca. 30 nm in diameter particles sticking well together. It is to be noted in this connection that, to avoid damage to electrical contacts and the entire structure of the IDA, the electrophoretic TiO<sub>2</sub> deposits did not undergo the usual high-temperature annealing but were simply dried at 100 °C. In fact, the deposition of colloidal TiO<sub>2</sub> coatings involves normally a final heating above 400 °C resulting in partial sintering of the nanoparticles.<sup>7</sup>

To evaluate the actual effect of the annealing temperature upon photoresponse of the TiO<sub>2</sub> films, we tested a series of electrophoretically deposited TiO<sub>2</sub> films supported on conventional size conducting glass samples. After being dried under ambient conditions, these TiO<sub>2</sub> deposits were heated in air at temperatures ranging from 100 to 500 °C. To avoid cracking

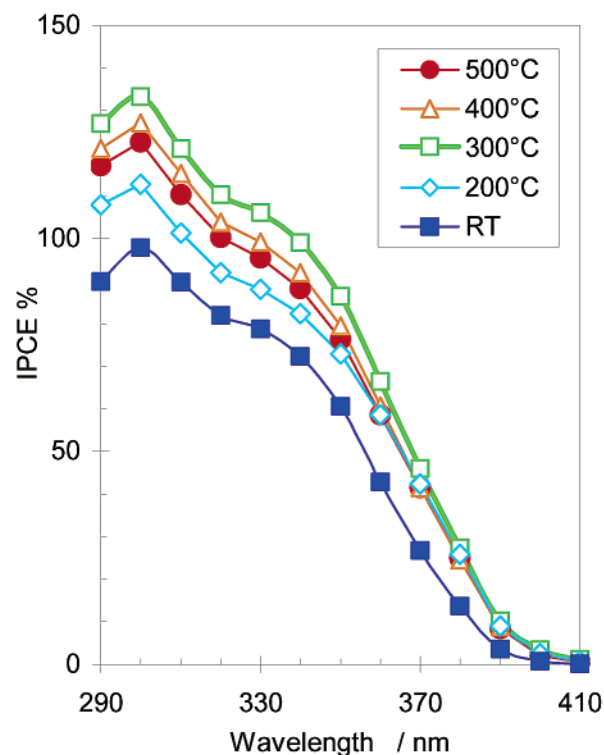


**Figure 3.** Spectral photoresponses, recorded in 0.1 M HCOOH/0.1 M HClO<sub>4</sub>, for a series of electrophoretically formed ca. 2  $\mu\text{m}$ -thick TiO<sub>2</sub> films annealed for 1 h at temperatures ranging from 200 to 500  $^{\circ}\text{C}$  and a film simply dried at room temperature. Exposed surface area of the film: 0.28 cm<sup>2</sup>.

during their annealing, we chose for this comparison relatively thin, ca. 2  $\mu\text{m}$  thick, TiO<sub>2</sub> films. Spectral photoresponses recorded in the presence of an efficient hole scavenger (in this case we chose formic acid) in the solution are shown in Figure 3. Interestingly, even a TiO<sub>2</sub> film just dried at room temperature exhibits already high incident photon-to-current conversion efficiencies (IPCEs) and the same shape of the spectral photoresponse as that observed for the sintered deposits. In addition, it is the film annealed at 300  $^{\circ}\text{C}$ , i.e., below the usual sintering temperature which exhibits the highest photoresponse.<sup>12</sup> It is also to be noted that the maximum of photocurrent efficiency, occurring for all films at ca. 300 nm, coincides with very short optical penetration depth ( $\alpha^{-1}$ )<sup>16</sup> about 3 orders of magnitude smaller than the actual film thickness. This implies quite clearly that even in the case of an unannealed film, the electric contacts between the TiO<sub>2</sub> nanoparticles established simply through the van der Waals–London interactions enable already an efficient charge transport to the back contact, across the unilluminated part of the film. As discussed elsewhere,<sup>12</sup> a possible explanation of the negligible effect of the sintering temperature upon the photoresponse of the TiO<sub>2</sub> film, consistent with low interparticle contact resistance, may lie in the self-doping of the mesoporous semiconducting structure taking place at the initial stages of the photocurrent flow.

In Figure 4 are displayed typical photocurrent–voltage curves for an interdigitated array of TiO<sub>2</sub> photoanodes irradiated with a 150 W Xe lamp through a neutral density filter of 40% transmission. The steep rise of the photocurrent, reaching a maximum already after application of a ca. 0.3 V anodic bias, is typical of the presence in the solution of an effective hole capture agent (in this case methanol), as previously observed using much larger (i.e., conventional size) electrodes consisting of sintered TiO<sub>2</sub> nanoparticles.<sup>17</sup> Interestingly, the clearly

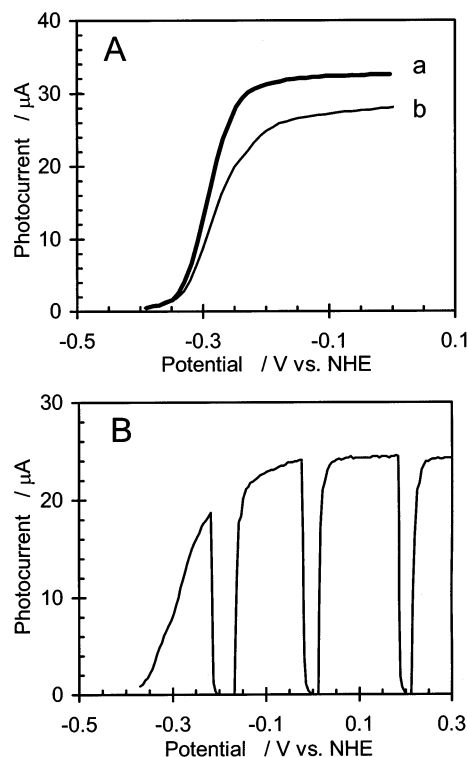


**Figure 4.** (A) Photocurrent–voltage curves for the oxidation of methanol (a deaerated 0.1 M aq. CH<sub>3</sub>OH solution) at an IDA of TiO<sub>2</sub> film microelectrodes, recorded in the absence (a) and in the presence (b) of a supporting electrolyte (1 M NaCl). Part B shows the  $i_{\text{ph}}$ – $E$  curve plotted under chopped light illumination.

perceptible difference in the amount of the photocurrent between curves a and b in Figure 4A reflects the effect of the supporting electrolyte.

In fact, while curve b was obtained in a 0.1 M CH<sub>3</sub>OH/1 M aq. NaCl solution, curve a was recorded in a solution of methanol in ultrapure water. Several series of measurements, involving different IDA TiO<sub>2</sub> electrodes, performed as a function of the concentration of supporting electrolyte (both NaCl and NaClO<sub>4</sub> were used for this purpose) confirmed a slight but consistent decrease of the photocurrent with increasing the ionic strength of the solution (Figure 5A and B). Such a trend appeared quite clearly when alternate measurements with largely differing concentrations of the supporting electrolyte were carried out (see also Figure 5B). In this regard close similarity between the dependence observed in NaCl and NaClO<sub>4</sub> solutions, respectively, points at the effect of ionic strength rather than that (specific) of an anion.

When considering possible reasons of the observed effect of the solution ionic strength upon the maximum photocurrent,<sup>18</sup> it is useful to recall that in the case of nanostructured TiO<sub>2</sub> electrodes the value of  $i_{\text{ph}}^{\text{max}}$  is affected not only by the incident light intensity but also by the rate of hole transfer to the species in the solution.<sup>12,17</sup> Thus, changes in the nature of hole scavenger present in the solution often result in largely differing maximum oxidation photocurrents. For example,  $i_{\text{ph}}^{\text{max}}$  associated with photooxidation of 0.1 M solution of methanol was found to be ca. 10 times larger than that corresponding to the photooxidation of water, but almost 2 times smaller than  $i_{\text{ph}}^{\text{max}}$  due to the photooxidation of formic acid.<sup>12</sup> Such a behavior is indicative of the persistence of the hole–electron ( $h^+/e^-$ ) recombination whatever the anodic bias, attributable to the absence of a regular space charge layer in the nanostructured TiO<sub>2</sub> electrodes.<sup>12,19</sup>



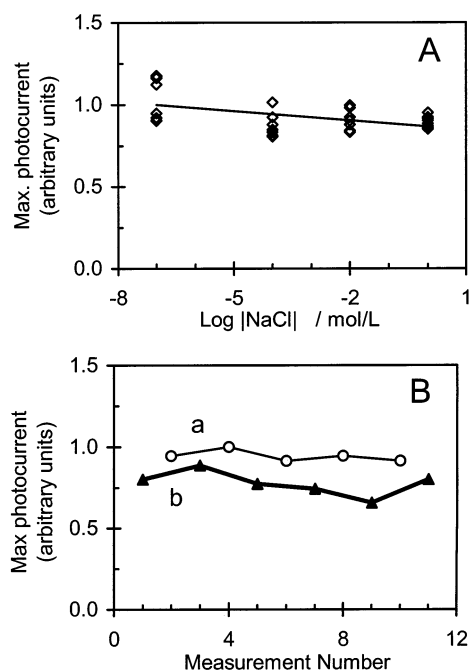
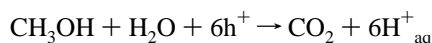


**Figure 5.** (A) Maximum saturation photocurrents recorded at an IDA of TiO<sub>2</sub> film microelectrodes in 1 M solution of CH<sub>3</sub>OH plotted as a function of concentration of the supporting electrolyte. Part (B) shows a series of alternate photocurrent measurements performed (a) in the absence and (b) in the presence of 1 mol/L of the supporting electrolyte.

The ability of hole capture agents to compete with the recombination processes may be affected by the solution pH. This is the case of methanol exhibiting higher photooxidation quantum efficiencies in alkaline and buffered neutral solutions than in acidic media.<sup>20</sup> As the photooxidation of methanol



produces one proton per every positive hole transferred, a pH gradient will develop close to the TiO<sub>2</sub> surface if the solution is not buffered. For the solution containing NaCl as supporting electrolyte, Cl<sup>-</sup> will act as counterion to H<sup>+</sup> ions formed at the TiO<sub>2</sub> photoanode, while Na<sup>+</sup> ions will play the same role toward OH<sup>-</sup> anions produced during water reduction at the cathode. However, in the case of interdigitated electrode configuration, development of large pH gradients will be, at least in part, prevented by the short diffusion path between the anode and cathode. Now, the absence of the supporting electrolyte creates an unusual situation in which a neutral reactant, CH<sub>3</sub>OH, undergoes oxidation in a solution containing initially only ions originating from the autoprotolysis of water and those due to accidental impurities. Under such conditions, the H<sup>+</sup> and OH<sup>-</sup> ions, generated at the anode and at the cathode, respectively, will be forced away from the electrodes by the combined effects of migration and diffusion. This suggests that the observed increase in the rate of methanol oxidation accompanying decreasing of ionic strength of the solution may be simply related to the easier withdrawal of H<sup>+</sup> ions (a coproduct of the photoanodic reaction) from the mesoporous TiO<sub>2</sub> electrode.

In fact, lowering the concentration of electrolyte will obviously affect the structure of the double layer at the TiO<sub>2</sub> interface, notably by increasing the characteristic thickness of the diffuse layer 1/κ (for a 1:1 electrolyte, 1/κ is proportional to the inverse square root of the ionic concentration).<sup>21</sup> Thus, for a 10<sup>-5</sup> M concentration of a 1:1 electrolyte in water at 25 °C 1/κ is already 96 nm and reaches 300 nm in a 10<sup>-6</sup> M

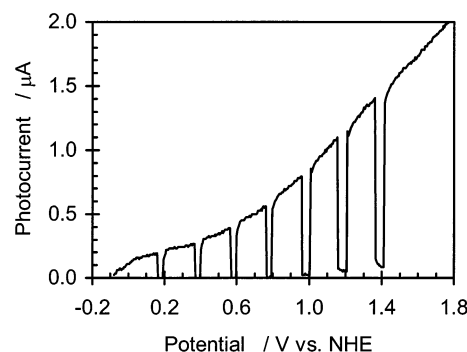


**Figure 6.** Photocurrent–voltage curve for the oxidation of ultrapure water at an IDA of TiO<sub>2</sub> microelectrodes recorded under chopped light illumination.

electrolyte. When comparing these values with the pore sizes in the TiO<sub>2</sub> film (cf. Figure 2B) it becomes evident that the ion atmospheres surrounding neighbor TiO<sub>2</sub> particles will interpenetrate. Assuming the surface of TiO<sub>2</sub> particles becomes positively charged under the photocurrent flow, the H<sup>+</sup> ions formed during the photoreaction will experience a net repulsion enhancing their migration outward of the film.

In view of the demonstrated ability of interdigitated TiO<sub>2</sub> microelectrodes to minimize resistive losses in the solution caused by the absence of the supporting electrolyte, we also attempted to photooxidize pure water. As shown in Figure 6, in that case the photocurrent increased rather slowly with the applied bias and, unlike for the methanol solution (cf. Figure 4), did not actually reach the saturation value.

Observation that the amount of the photocurrent measured in relatively concentrated (e.g., 1 M) solutions of various effective hole scavengers, such as methanol, still increased with further addition of the reactant prompted us to extend investigations to a large range of concentrations including almost pure reactants. In particular, various series of measurements were conducted with methanol solutions, both in pure water and in the presence of supporting electrolyte. Curve a in Figure 7A shows a typical plot of the maximum photocurrent recorded at the IDA of TiO<sub>2</sub> microelectrodes (irradiated with a 150 W Xe lamp through a 40% neutral density filter) as a function of the amount of methanol present in the solution. The represented data were collected in a series of carefully deaerated solutions of methanol in 0.1 M aq. HClO<sub>4</sub>. Closely similar relationship was also obtained using solutions of methanol in ultrapure water. Interestingly, the corresponding  $i_{\text{ph}}^{\text{max}}$  values increase, first rapidly and then steadily, with increasing the methanol concentration up to 99% v/v (since water serves as electroactive species at the IDA cathodes we did not attempt to use pure methanol). As the observed dependence, extending over such large composition range, can hardly be attributed to mass transport limitations, this strongly suggests that the rate of methanol photooxidation, under such moderate illumination, is governed by its extent of coverage of the TiO<sub>2</sub> surface. It is to be recalled, in this connection, that the adsorption of electroactive species is considered as a prerequisite for the photooxidation reaction to proceed via a direct hole transfer.<sup>3,22</sup> Although it remains unclear to what extent the methanol adsorption, favoring photooxidation via mobile holes, involves competition with water molecules for active sites on the TiO<sub>2</sub> surface, the plot shown in part A of Figure 7 strongly suggests that the surface becomes saturated only in pure methanol. The adsorption of methanol onto hydroxylated TiO<sub>2</sub> (rutile) surface has been reported to involve replacement of molecular water and interac-

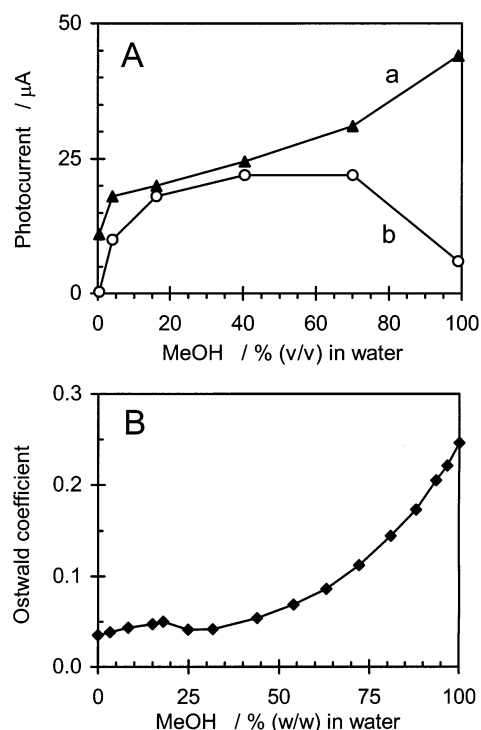
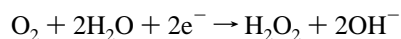


**Figure 7.** (A) Saturation photocurrents recorded at an IDA of TiO<sub>2</sub> microelectrodes in a series of deaerated (curve a) and air-saturated (curve b) methanol/water solutions. (B) Solubility of oxygen in water/methanol solutions, represented as the Ostwald coefficient (i.e.,  $V_{O_2}/V_{\text{solution}}$ ). Data taken from ref 27.

tion with surface OH groups.<sup>23</sup> With increasing the concentration of “free” OH groups on the TiO<sub>2</sub> surface, in diluted methanol solutions, photooxidation via trapped holes, i.e., surfaces bound •OH radicals<sup>24</sup> may become a significant reaction pathway.

The fact that similar dependence of maximum photoanodic current on methanol concentration was also observed in the case of conventional size photoelectrodes (ca. 2.5 μm-thick nanostructured TiO<sub>2</sub> films supported on conducting glass) rules out any specific effect of film thickness. However, in the latter case, the photocurrent–voltage curves recorded in concentrated methanol solutions were clearly affected by uncompensated ohmic drop in the solution, reaching a plateau only at relatively large anodic bias.

Photoresponse of the interdigitated TiO<sub>2</sub> microelectrodes was particularly sensitive to the presence of oxygen in the solution. Figure 8A displays photocurrent–voltage curves obtained for the oxidation of 0.1 M solution of methanol in water either deaerated or saturated with air or with oxygen. Apparently, the observed dramatic effect of dissolved oxygen is mainly due to the specific IDA configuration where the cathodic microbands, at which oxygen reduction is expected to take place, are only 5 μm distant from the TiO<sub>2</sub> microanodes. In fact, addition of  $2.5 \times 10^{-3}$  mol/L of H<sub>2</sub>O<sub>2</sub> (an amount close to the solubility of O<sub>2</sub>) to the methanol solution resulted practically in a suppression of the photocurrent (cf. Figure 8B). This suggests that H<sub>2</sub>O<sub>2</sub> formed via the O<sub>2</sub> reduction at the microcathode



will act as a more effective scavenger of conduction band electrons at the TiO<sub>2</sub> microanode than oxygen itself.<sup>25</sup> Interestingly, the extent to which oxygen affected the anodic photocurrent depended clearly upon methanol concentration in the solution (cf. curve b in Figure 7A). First, the ratio of the

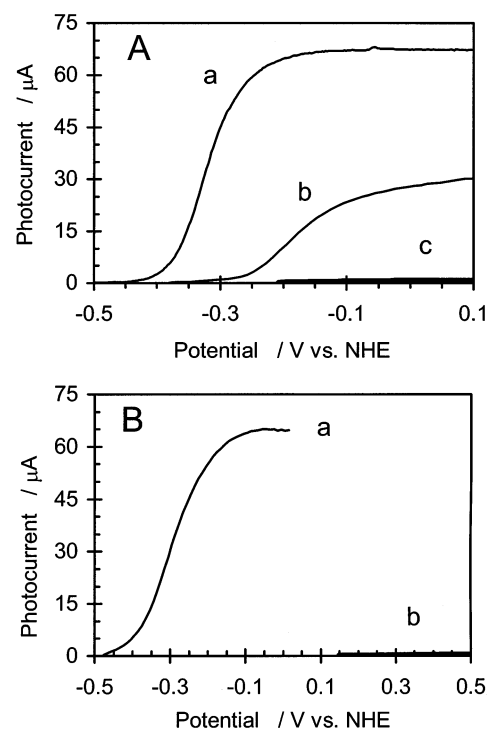


**Figure 8.** (A) Photocurrent–voltage curves for the oxidation of methanol at an IDA of TiO<sub>2</sub> microelectrodes recorded in (a) deaerated, (b) air-saturated, (c) O<sub>2</sub>-saturated 0.1 M CH<sub>3</sub>OH solution in water. (B) As in part (A): in the presence (b) and in the absence (a) of  $2.5 \times 10^{-3}$  M of H<sub>2</sub>O<sub>2</sub> in a deaerated 0.1 M CH<sub>3</sub>OH solution.

photocurrents in deaerated versus air-saturated solution decreased with increasing methanol concentration, but the trend became opposite at very large methanol concentrations. This result reflects the competition for the adsorption sites at the TiO<sub>2</sub> surface between methanol, on the one side, and hydrogen peroxide and/or oxygen, on the other. It is the high solubility of oxygen in methanol-rich mixtures with water (cf. Figure 7B) which should be the cause of the decrease of the net photocurrent occurring in the latter range of concentrations. As both oxygen and hydrogen peroxide have been reported to enhance the yield of reacting holes in photocatalytic reactions,<sup>26</sup> the O<sub>2</sub>- and H<sub>2</sub>O<sub>2</sub>-induced decrease of the net photocurrent is to be assigned principally to a change in the mode of operation of the TiO<sub>2</sub> film. In fact, the TiO<sub>2</sub> film, acting exclusively as a photoanode in the deaerated solution of methanol, becomes apparently, in the presence of oxygen, the site of a combined CH<sub>3</sub>OH oxidation/O<sub>2</sub> and H<sub>2</sub>O<sub>2</sub> reduction process. Ability of the anodically polarized nanostructured TiO<sub>2</sub> films to operate in a “photocatalytic mode”, like a colloidal suspension of semiconductor particles, (consistent with our preliminary mass balance assessments) raises clearly the question of the actual potential distribution across such films.

As already mentioned, the value of maximum photocurrent observed at a nanostructured TiO<sub>2</sub> electrode reflects directly the photoanodic activity of a given electron donor. In principle, we do not include in such a comparison reversible and quasi-reversible redox couples where the product of photooxidation reaction may act as scavenger of photogenerated conduction-band electrons. This kind of “redox cycling”, observed, for example, for such couples as hydroquinone/quinone, I<sup>−</sup>/I<sub>3</sub><sup>−</sup>, and also H<sub>2</sub>O/O<sub>2</sub>, results in an effective h<sup>+</sup>/e<sup>−</sup> recombination and in a dramatic decrease of the photocurrent. The situation is quite different for the majority of organic species, undergoing an irreversible photooxidation, the products of which (e.g., CO<sub>2</sub>, H<sup>+</sup><sub>aq</sub> ions) are reduced only extremely slowly at the surface of

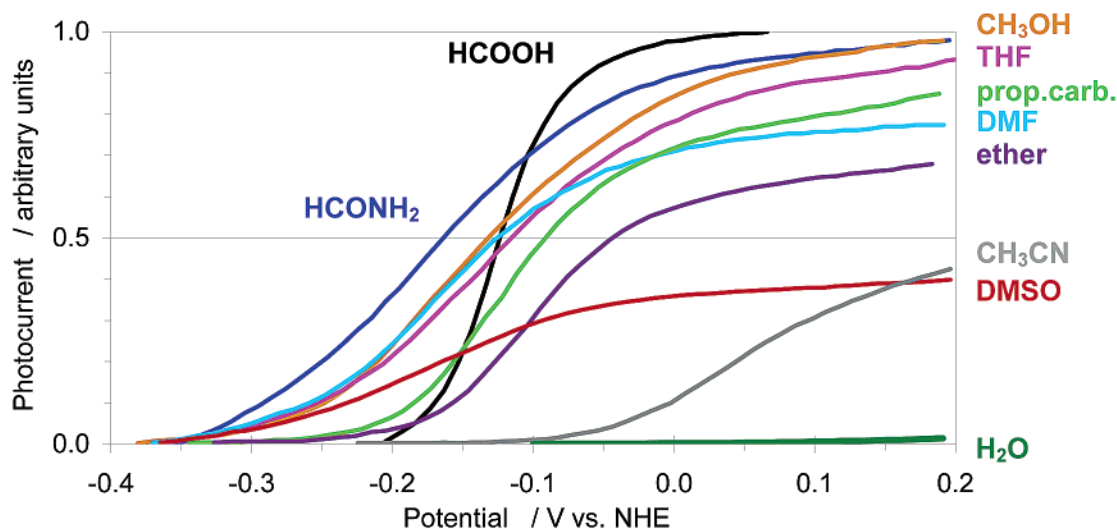


**Figure 9.** Photocurrent–voltage curves recorded at an IDA of TiO<sub>2</sub> film microelectrodes in deaerated 1 M aq. solutions of the following organic substrates: formic acid, formamide (H<sub>2</sub>NCHO), methanol, THF (tetrahydrofuran), propylene carbonate, DMF (*N,N*-dimethylformamide), diethyl ether, DMSO (dimethyl sulfoxide), acetonitrile.

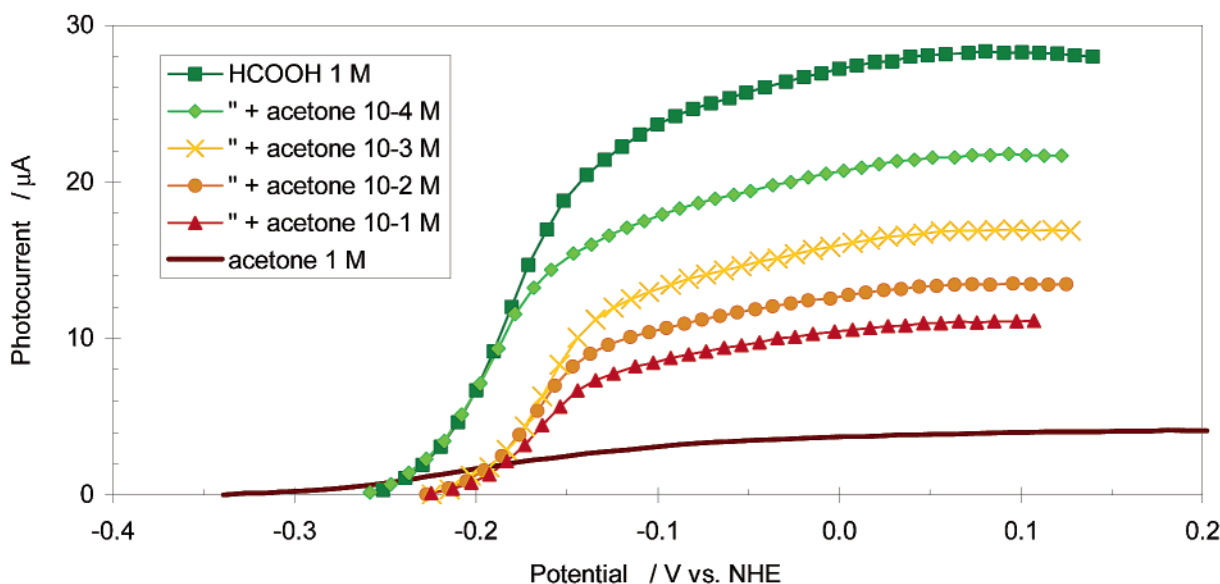


**Figure 10.** Effect of successive acetone additions to a deaerated 1 M HCOOH solution in water upon photoresponse of an IDA of TiO<sub>2</sub> microelectrodes.

TiO<sub>2</sub>. In such a case (and providing there are no other electron scavengers in the solution), the value of  $i_{ph}^{max}$  reflects the competition between the interfacial hole transfer and the  $h^+/e^-$  recombination.

The plots shown in Figure 9 represent the dependence of photoanodic current on applied bias for a series of 1 M solutions of organic compounds (most of them used as solvents) in ultrapure water. Some of these compounds, formamide, THF, and DMF, appear as photoactive as formic acid or methanol considered as particularly efficient hole scavengers. Slow initial rise of the photocurrent observed in the solutions of propylene carbonate, ether, and particularly acetonitrile may be indicative of a partial blocking of the TiO<sub>2</sub> surface by the reactant itself or by its photooxidation intermediates. Importantly, all these organic compounds are oxidized preferentially with respect to water, with the notable exceptions of acetone and acetophenone. The latter caused practically a suppression of the photocurrent (the  $i_{ph}$  values observed after addition of ca. 0.6 mol/L of acetophenone were at least 20 times smaller than those determined in pure water, represented by the  $i_{ph}$ – $E$  plot close

to the X-axis of Figure 9). The case of acetophenone may be similar to that of strongly adsorbed chlorohydroxybenzoic acid for which the rates of photocatalytic degradation in aerated aqueous suspensions of TiO<sub>2</sub> (P25) were unexpectedly low and decreased with increasing concentration of the pollutant in water.<sup>4</sup> The partial inhibition of the photooxidation process by the strongly adsorbed reactant (or its photodegradation product) has been explained in terms of the blockage of active sites on the TiO<sub>2</sub> surface resulting in a depletion of surface OH groups and also in a decreased turnover of the reactant itself.<sup>4</sup> An impeding effect of strongly adsorbed reactant or photoproduct upon the electron-scavenging process, i.e., the oxygen reduction, may be yet another reason.

In this regard, the IDAs of TiO<sub>2</sub> microelectrodes offer the possibility to discriminate not only between the anodic and cathodic effects but also between the blockage of the TiO<sub>2</sub> surface either by the reactant or by its photooxidation product. They appear also particularly suitable for monitoring photooxidation reactions involving substrates of differing adsorption strengths and hole capture kinetics. This kind of situation is

illustrated by the series of photocurrent–voltage curves represented in Figure 10, showing the effect of addition of increasing amounts of acetone upon photooxidation of formic acid. The saturation photocurrent recorded in a 1 M solution of HCOOH (an efficient hole scavenger) was already visibly affected by the addition of  $10^{-4}$  mol/L of acetone, consistent with its effective blocking of active sites at the TiO<sub>2</sub> surface.

## Conclusions

As shown by the measurements performed using arrays of microelectrodes, the charge transport in nanostructured TiO<sub>2</sub> films is very little affected by the ionic strength of the electrolyte. Manifestly, the H<sup>+</sup> ions formed in the course of the photooxidation process (e.g., of methanol) are already enough to ensure efficient screening of the electrons moving to the back contact. The demonstrated ability of the IDA of TiO<sub>2</sub> microelectrodes to operate reliably in low conductivity media, including solutions of uncharged reactants in ultrapure water, allows one, in particular, to follow the photooxidation reactions in the absence of ions of a supporting electrolyte, affecting in many cases adsorption of organic compounds on the TiO<sub>2</sub> particles. As shown in the case of methanol (employed here as a model hole scavenger), under moderate irradiation, the reactant adsorption on active sites of the photocatalyst appears as the rate-determining step of the photooxidation process. The observed continuous increase of the photocurrent with increasing the methanol/water ratio is consistent with the photooxidation reaction occurring (at least in concentrated methanol solutions) via a direct hole transfer.

The specific configuration of the IDA, with the microanodes and microcathodes spaced only 5  $\mu$ m apart, allowed us to study the local effect of the cathodic reduction of oxygen upon amount of the anodic photocurrent associated with the oxidation of methanol. We assign the observed decrease of the photocurrent to the effect of hydrogen peroxide generated at the microcathodes rather than to that of the oxygen itself. In fact, the presence of oxygen in the solution affected much less the anodic photocurrent when the local microcathodes were replaced by a conventional macrocathode. We tentatively suggest that the above-mentioned decrease of the photocurrent is due to the scavenging of the conduction band electrons in TiO<sub>2</sub> by hydrogen peroxide, leading to a partial substitution of the purely anodic process (with the collection of the electrons at the back contact) by a combined anodic/cathodic process similar to that occurring in irradiated suspensions of the semiconductor particles.

Comparative photocurrent–voltage measurements performed in aqueous solutions of various organic compounds (usually employed as solvents) revealed a wide spectrum of activities toward oxidation at a TiO<sub>2</sub> photoanode. Although most of them act as effective hole scavengers, almost as active as formic acid and methanol, others, such as acetone and especially acetophenone, cause a virtual suppression of the photocurrent. The fact that the photocurrents associated with the oxidation of such effective hole scavengers as formic acid or methanol are markedly affected by the addition to the solution of even small amounts of either acetone or acetophenone indicates clearly the strong preferential adsorption of the latter compounds causing blocking of the active sites on the surface of TiO<sub>2</sub> nanoparticles. In view of these results, the IDA of TiO<sub>2</sub> microelectrodes appear as an efficient tool for identifying such surface blocking interactions often affecting the efficiency of photocatalytic detoxification processes.

**Acknowledgment.** This research was supported by the Swiss National Science Foundation.

## References and Notes

- (1) *Photocatalytic Purification and Treatment of Water and Air*; Ollis, D. F., Al-Ekabi, H., Eds.; Elsevier: Amsterdam, 1993; Pichat, P. *Catal. Today* **1994**, *19*, 313–333; Bahnemann, D.; Cunningham, J.; Fox, M. A.; Pelizzetti, E.; Pichat, P.; Serpone, N. *Aquat. Surf. Photochem.* **1994**, 261–316.
- (2) Hoffmann, M. R.; Martin, S. T.; Choi, W. Y.; Bahnemann, D. W. *Chem. Rev.* **1995**, *95*, 69–96.
- (3) Fox, M. A.; Dulay, M. T. *Chem. Rev.* **1993**, *93*, 341–357.
- (4) Cunningham, J.; Al-Sayyed, G.; Sedlak, P.; Caffrey, J. *Catal. Today* **1999**, *53*, 145–158.
- (5) Tomkiewicz, M. *Catal. Today* **2000**, *58*, 115–123.
- (6) Heller, A. *Acc. Chem. Res.* **1995**, *28*, 503–508.
- (7) O'Regan, B.; Gratzel, M. *Nature* **1991**, *353*, 737–740.
- (8) Hagfeldt, A.; Graetzel, M. *Acc. Chem. Res.* **2000**, *33*, 269–277; Gratzel, M. *Nature (London)* **2001**, *414*, 338–344.
- (9) Vanmaekelbergh, D.; deJongh, P. E. *J. Phys. Chem. B* **1999**, *103*, 747–750; Sodergren, S.; Hagfeldt, A.; Olsson, J.; Lindquist, S. E. *J. Phys. Chem.* **1994**, *98*, 5552–5556; Cao, F.; Oskam, G.; Searson, P. C. *J. Phys. Chem.* **1996**, *100*, 17021–17027; Schlichthoerl, G.; Huang, S. Y.; Sprague, J.; Frank, A. J. *J. Phys. Chem. B* **1997**, *101*, 8139–8153; Bond, A. M.; Deacon, G. B.; Howitt, J.; MacFarlane, D. R.; Spiccia, L.; Wolfbauer, G. *J. Electrochem. Soc.* **1999**, *146*, 648–656; Dloczik, L.; Ieperuma, O.; Lauermaier, I.; Peter, L. M.; Ponomarev, E. A.; Redmond, G.; Shaw, N. J.; Uhlendorf, I. *J. Phys. Chem. B* **1997**, *101*, 10281–10289; Nelson, J. *Phys. Rev. B: Condens. Matter Mater. Phys.* **1999**, *59*, 15374–15380; Papa-georgiou, N.; Graetzel, M.; Infelta, P. P. *Sol. Energy Mater. Sol. Cells* **1996**, *44*, 405–438; O'Regan, B.; Moser, J.; Anderson, M.; Graetzel, M. *J. Phys. Chem.* **1990**, *94*, 8720–8726.
- (10) Solbrand, A.; Lindstrom, H.; Rensmo, H.; Hagfeldt, A.; Lindquist, S. E.; Sodergren, S. *J. Phys. Chem. B* **1997**, *101*, 2514–2518.
- (11) Brus, L. *Phys. Rev. B: Condens. Matter* **1996**, *53*, 4649–4656.
- (12) Wahl, A.; Augustynski, J. *J. Phys. Chem. B* **1998**, *102*, 7820–7828.
- (13) Niwa, O. *Electroanalysis* **1995**, *7*, 606–613.
- (14) Augustynski, J. *Struct. Bonding* **1988**, *69*, 1–61.
- (15) Fiacabrino, G. C.; Koudelka-Hep, M. *Electroanalysis* **1998**, *10*, 217–222.
- (16) Eagles, D. M. *J. Phys. Chem. Solids* **1964**, *25*, 1243–1251.
- (17) Wahl, A.; Ulmann, M.; Carroy, A.; Augustynski, J. *J. Chem. Soc. Chem. Commun.* **1994**, 2277–2278.
- (18) We wish to point out, in this connection, that the present situation involving oxidation at a photoanode of a neutral electroactive species, such as methanol, is totally different from that concerning the reduction/oxidation of cations/anions at an electrode. In fact, in the latter case, the well-known increase of the polarographic limiting currents, due to the discharge of a metal cation, when decreasing the concentration of the supporting electrolyte is simply related to the migration-assisted transport of the electroactive species to the cathode. Lingane, J. J.; Kolthoff, I. M. *J. Am. Chem. Soc.* **1939**, *61*, 1045.
- (19) Santato, C.; Ulmann, M.; Augustynski, J. *Adv. Mater.* **2001**, *13*, 511–514.
- (20) Wahl, A.; Ulmann, M.; Carroy, A.; Jermann, B.; Dolata, M.; Kedzierzawski, P.; Chatelain, C.; Monnier, A.; Augustynski, J. *J. Electroanal. Chem.* **1995**, *396*, 41–51.
- (21) Bard, A. J.; Faulkner, L. R. *Electrochemical Methods: Fundamentals and Applications*; John Wiley & Sons: New York, 1980.
- (22) Matthews, R. W. *J. Catal.* **1988**, *113*, 549.
- (23) Nakamura, R.; Ueda, K.; Sato, S. *Langmuir* **2001**, *17*, 2298–2300; Suda, Y.; Morimoto, T.; Nagao, M. *Langmuir* **1987**, *3*, 99–104.
- (24) Lawless, D.; Serpone, N.; Meisel, D. *J. Phys. Chem.* **1991**, *95*, 5166–5170; Minero, C.; Catozzo, F.; Pelizzetti, E. *Langmuir* **1992**, *8*, 481–486.
- (25) Measurements involving anodic polarization of the TiO<sub>2</sub> microanodes in air-saturated methanol solutions against a few millimeter distant external cathode (instead of the local microcathodes) showed only a slight decrease of the photocurrents in comparison with those in deaerated solutions.
- (26) Wei, T. Y.; Wang, Y. Y.; Wan, C. C. *J. Photochem. Photobiol., A* **1990**, *55*, 115–126; Tanaka, K.; Hisanaga, T.; Rivera, A. P. *Trace Met. Environ.* **1993**, *3*, 169–178; Goldstein, S.; Czapski, G.; Rabani, J. *J. Phys. Chem.* **1994**, *98*, 6586–6591; Sun, L.; Bolton, J. R. *J. Phys. Chem.* **1996**, *100*, 4127–4134.
- (27) Tokunaga, J. *J. Chem. Eng. Data* **1975**, *20*, 41–46.